Supplementary Information for:

Exploring Dominant Strategies in Evolutionary Games: A Multi-Agent Reinforcement Learning Approach

Supplementary Note 1: The detailed formulation of MTBR

The complete formulation of the memory-two bilateral reciprocity (MTBR) strategy is delineated in Supplementary Table 1.

To understand why the table has 20 rows, we need to consider the total number of possible states (N_{state}) in a two-step memory framework. This calculation is more complex than it might initially appear, due to the varying number of states in the initial rounds where full history is not yet available.

Let's break down the calculation:

1. There are 2 individuals, each having $M = 2$ possible actions (cooperate or defect).

2. The maximum memory length is $\ell = 2$.

3. At each interaction step, there are $M \times M = 4$ possible outcomes.

4. However, we need to consider the initial rounds where agents do not have a full history of ℓ steps: - In the first round: 1 state (initial state) - In the second round: $M^2 = 4$ states - From the third round onwards: $M^{2\ell} = 16$ states.

Therefore, the total number of possible states is the sum of all these possibilities:

$N_{state} = 1 + M^2 + M^{2\ell} = 1 + 4 + 16 = 21$.

This sum can be generalized and expressed as a geometric series: $N_{state} = (\frac{M^{2\ell+2}-1}{M^2-1} - 1)$.

For MTBR with $M = 2$ and $\ell = 2$: $N_{state} = (\frac{2^{2(2)+2}-1}{2^2-1} - 1) = (\frac{63}{3} - 1) = 20$.

This table comprehensively outlines the decision-making processes under a two-step memory framework, presenting each possible state and corresponding strategic responses according to the MTBR's Q-table. Supplementary Table 1 is essential for replicating our findings and understanding the nuanced behavior of agents within the simulated Markov game environments discussed in our study.

Supplementary Note 2: Theoretical analysis

Interaction

We consider the evolutionary dynamics of n strategies, labeled in $1, \cdots, n$, in a well-mixed population of finite and fixed size N. The payoff of these individuals depends on their counterpart's strategies and the payoff matrix

	s_1	s_2	$\cdots$	s_n
s_1	a_{11}	a_{12}	$\cdots$	a_{1n}
s_2	a_{21}	a_{22}	$\cdots$	a_{2n}
$\vdots$	$\vdots$	$\vdots$	$\ddots$	$\vdots$
s_n	a_{n1}	a_{n2}	$\cdots$	a_{nn}

where a_{ij} denotes the payoff received by an i-individual subsequent to the interaction with a j-player. Define the number of i-individuals as X_i and the state vector $\mathbf{X} = (X_1, X_2, \cdots, X_n)$. We know $\sum_{k=1}^{n} X_k = N$. Therefore, we obtain the average payoff of i-individuals

$$\bar{U}_i(\mathbf{X}) = \frac{1}{N-1}\left(a_{i1}X_1 + \cdots + a_{ii}(X_i - 1) + \cdots + a_{in}X_n\right), \tag{1}$$

and the average payoff of all players

$$\bar{U}(\mathbf{X}) = \frac{1}{N}\left(\sum_{k=1}^{n} \bar{U}_i(\mathbf{X})X_k\right). \tag{2}$$

Strategy updates

After all interactions, a random player i is selected to update his strategy, and another random player j is selected. Player i imitates player j's strategy with probability

$$p_{i\to j} = \frac{1}{1 + \exp\left(\delta\left(\bar{U}_i - \bar{U}_j\right)\right)}. \tag{3}$$

Under weak selection, the probability can be expanded as

$$p_{i\to j} = \frac{1}{2} + \delta\frac{\bar{U}_j - \bar{U}_i}{4} + O(\delta^2). \tag{4}$$

The probability that the number of i-individual increases from X_i to $X_i + 1$ is

$$T_i^+(\mathbf{X}) = \sum_{j \neq i} p_{j \to i} \frac{X_i X_j}{N(N-1)}, \tag{5}$$

whereas probability that the number of i-individual decreases from X_i to $X_i - 1$ is

$$T_i^-(\mathbf{X}) = \sum_{j \neq i} p_{i \to j} \frac{X_i X_j}{N(N-1)}. \tag{6}$$

Under weak selection, we can rewrite the equations as

$$T_i^+(\mathbf{X}) = \sum_{j \neq i} \left(\frac{1}{2} + \delta \frac{\bar{U}_i - \bar{U}_j}{4} \right) \frac{X_i X_j}{N(N-1)}, \tag{7}$$

$$T_i^-(\mathbf{X}) = \sum_{j \neq i} \left(\frac{1}{2} + \delta \frac{\bar{U}_j - \bar{U}_i}{4} \right) \frac{X_i X_j}{N(N-1)}. \tag{8}$$

Evolutionary dynamics

The stochastic evolution process can be formulated in terms of the master equation

$$\begin{aligned} P^{\tau+1}(\mathbf{X}) - P^{\tau}(\mathbf{X}) = & \sum_{i=1}^{n} P^{\tau}(X_1, \cdots, X_i - 1, \cdots, X_n) T^+(X_1, \cdots, X_i - 1, \cdots, X_n) \\ & + \sum_{i=1}^{n} P^{\tau}(X_1, \cdots, X_i + 1, \cdots, X_n) T^-(X_1, \cdots, X_i + 1, \cdots, X_n) \\ & - \sum_{i=1}^{n} P^{\tau}(\mathbf{X}) T^+(\mathbf{X}) - \sum_{i=1}^{n} P^{\tau}(\mathbf{X}) T^-(\mathbf{X}), \end{aligned} \tag{9}$$

where $P^{\tau}(\mathbf{X})$ is the probability that the system is in state $\mathbf{X}$ at time τ. Introducing the notation $x_i = X_i/N$, $\mathbf{x} = \mathbf{X}/N$, $t = \tau/N$, and the probability density function $\rho(\mathbf{x}, t) = NP^{\tau}(\mathbf{X})$

yields

$$
\begin{aligned}
&\rho\left(\mathbf{x}, t+N^{-1}\right)-\rho(\mathbf{x}, t) \\
=&\sum_{i=1}^{n} \rho\left(x_1, \cdots, x_i-N^{-1}, \cdots, x_n, t\right) T_i^{+}\left(x_1, \cdots, x_i-N^{-1}, \cdots, x_n\right) \\
&+\sum_{i=1}^{n} \rho\left(x_1, \cdots, x_i+N^{-1}, \cdots, x_n, t\right) T_i^{-}\left(x_1, \cdots, x_i+N^{-1}, \cdots, x_n\right) \\
&-\sum_{i=1}^{n} \rho(\mathbf{x}, t) T_i^{-}(\mathbf{x})-\sum_{i=1}^{n} \rho(\mathbf{x}, t) T_i^{+}(\mathbf{x}) .
\end{aligned}
\tag{10}
$$

The probability density function and the transition probability can be expanded in a Taylor series at $(\mathbf{x}, t)$ for large N. Negelecting high order terms in N^{-1}, we get

$$
\begin{aligned}
&\frac{1}{N} \frac{\partial}{\partial t} \rho(\mathbf{x}, t) \\
=&\sum_{i=1}^{n}\left(\rho(\mathbf{x}, t)-\frac{1}{N} \frac{\partial}{\partial x_i} \rho(\mathbf{x}, t)+\frac{1}{2 N^2} \frac{\partial^2}{\partial x_i^2} \rho(\mathbf{x}, t)\right)\left(T_i^{+}(\mathbf{x})-\frac{1}{N} \frac{\partial}{\partial x_i} T_i^{+}(\mathbf{x})+\frac{1}{2 N^2} \frac{\partial^2}{\partial x_i^2} T_i^{+}(\mathbf{x})\right) \\
&+\sum_{i=1}^{n}\left(\rho(\mathbf{x}, t)+\frac{1}{N} \frac{\partial}{\partial x_i} \rho(\mathbf{x}, t)+\frac{1}{2 N^2} \frac{\partial^2}{\partial x_i^2} \rho(\mathbf{x}, t)\right)\left(T_i^{-}(\mathbf{x})+\frac{1}{N} \frac{\partial}{\partial x_i} T_i^{-}(\mathbf{x})+\frac{1}{2 N^2} \frac{\partial^2}{\partial x_i^2} T_i^{-}(\mathbf{x})\right) \\
&-\sum_{i=1}^{n} \rho(\mathbf{x}, t) T_i^{-}(\mathbf{x})-\sum_{i=1}^{n} \rho(\mathbf{x}, t) T_i^{+}(\mathbf{x}) \\
=&-\frac{1}{N} \sum_{i=1}^{n} \frac{\partial}{\partial x_i}\left(\phi_i(\mathbf{x}) \rho(\mathbf{x}, t)\right)+\frac{1}{2 N} \sum_{i=1}^{n} \frac{\partial^2}{\partial x_i^2}\left(\psi_i^2(\mathbf{x}) \rho(\mathbf{x}, t)\right) .
\end{aligned}
\tag{11}
$$

Finally, we obtain

$$
\frac{\partial}{\partial t} \rho(\mathbf{x}, t)=-\sum_{i=1}^{n} \frac{\partial}{\partial x_i}\left(\phi_i(\mathbf{x}) \rho(\mathbf{x}, t)\right)+\sum_{i=1}^{n} \frac{\partial^2}{\partial x_i^2}\left(\psi_i^2(\mathbf{x}) \rho(\mathbf{x}, t)\right), \tag{12}
$$

where

$$
\phi_i(\mathbf{x})=T_i^{+}(\mathbf{x})-T_i^{-}(\mathbf{x})=\frac{\delta N}{2(N-1)} x_i\left(\bar{U}_i-\bar{U}\right), \tag{13a}
$$

$$
\psi_i(\mathbf{x})=\sqrt{\left(T_i^{+}(\mathbf{x})+T_i^{-}(\mathbf{x})\right) / N}=\sqrt{x_i(1-x_i) /(N-1)}. \tag{13b}
$$

The partial differential equation has the form of a Fokker-Planck equation. Meanwhile, we can derive the corresponding Langevin equation

$$\dot{x}_i = \phi_i(\mathbf{x}) + \psi_i(\mathbf{x})\xi, \tag{14}$$

where ξ is the Gaussian noise.

Equilibrium point

The equilibrium points are determined by the first term of Eq. 14, while the second term affects the stability. To find all equilibrium points, we can omit the second term and let $\dot{x}_i = 0$ for all $i \in \{1, 2, \cdots, n\}$, from which we know there are n boundary equilibrium points $(1, 0, \cdots 0), (0, 1, \cdots, 0), \cdots, (0, 0, \cdots, 1)$. In scenarios where interior equilibrium points exist, we discuss the following cases.

All strategies coexist

In this case, the following equations must hold

$$\bar{U}_1(\mathbf{x}) = \bar{U}_2(\mathbf{x}) = \cdots = \bar{U}_n(\mathbf{x}), \tag{15a}$$

$$x_1 + x_2 + \cdots + x_n = 1. \tag{15b}$$

Moreover, we get a system of linear equations

$$\begin{cases} x_1(a_{11} - a_{21}) + x_2(a_{12} - a_{22}) + \cdots + x_n(a_{1n} - a_{2n}) = \dfrac{a_{11} - a_{22}}{N}, \\ x_1(a_{11} - a_{31}) + x_2(a_{12} - a_{32}) + \cdots + x_n(a_{1n} - a_{3n}) = \dfrac{a_{11} - a_{33}}{N}, \\ \vdots \qquad\qquad \vdots \qquad\qquad \vdots \\ x_1(a_{11} - a_{n1}) + x_2(a_{12} - a_{n2}) + \cdots + x_n(a_{1n} - a_{nn}) = \dfrac{a_{11} - a_{nn}}{N}, \\ x_1 + \qquad x_2 + \cdots + \qquad x_n = 1, \end{cases} \tag{16}$$

where $0 < x_i < 1, \forall i \in \{1, 2, \cdots, n\}$. Rewrite these equations in the matrix form

$$\mathbf{A}\mathbf{x} = \mathbf{b}, \tag{17}$$

where

$$\mathbf{A} = \begin{pmatrix} a_{11} - a_{21} & a_{12} - a_{22} & \cdots & a_{1n} - a_{2n} \\ a_{11} - a_{31} & a_{12} - a_{32} & \cdots & a_{1n} - a_{3n} \\ \vdots & \vdots & \ddots & \vdots \\ a_{11} - a_{n1} & a_{12} - a_{n2} & \cdots & a_{1n} - a_{nn} \\ 1 & 1 & \cdots & 1 \end{pmatrix}, \tag{18}$$

$$\mathbf{b} = \begin{pmatrix} (a_{11} - a_{22})/N \\ (a_{11} - a_{33})/N \\ \vdots \\ (a_{11} - a_{nn})/N \\ 1 \end{pmatrix}. \tag{19}$$

Therefore, if $|\mathbf{A}| \neq 0$ holds, there may exist an interior equilibrium point. According to the Cramer's rule, we obtain

$$\begin{aligned} x_1 &= \frac{|\mathbf{A}_1|}{|\mathbf{A}|}, \\ x_2 &= \frac{|\mathbf{A}_2|}{|\mathbf{A}|}, \\ &\vdots \\ x_n &= \frac{|\mathbf{A}_n|}{|\mathbf{A}|}, \end{aligned} \tag{20}$$

where $\mathbf{A}_i$ is the matrix formed by replacing the i_{th} column of $\mathbf{A}$ by the column vector $\mathbf{b}$.

m strategies coexist

Denote the fraction of remaining strategies as $x_{i_1}, x_{i_2}, \cdots, x_{i_m}$ and the fraction of the extinct strategies $x_{j_1}, x_{j_2}, \cdots, x_{j_{n-m}}$. Let $\mathcal{I} := \{i_1, i_2, \cdots, i_m\}$ and $\mathcal{J} := \{j_1, j_2, \cdots, j_m\}$. In this case, the following equations must hold

$$\bar{U}_{i_1}(\mathbf{x}) = \bar{U}_{i_2}(\mathbf{x}) = \cdots = \bar{U}_{i_m}(\mathbf{x}), \tag{21a}$$

$$x_{i_1} + x_{i_2} + \cdots + x_{i_m} = 1, \tag{21b}$$

$$x_{j_1} = x_{j_2} = \cdots = x_{j_{n-m}} = 0. \tag{21c}$$

Similarly, we get a system of linear equations

$$\begin{cases} x_{i_1}(a_{i_1i_1} - a_{i_2i_1}) + x_{i_2}(a_{i_1i_2} - a_{i_2i_2}) + \cdots + x_{i_m}(a_{i_1i_m} - a_{i_2i_m}) = \dfrac{a_{i_1i_1} - a_{i_2i_2}}{N}, \\ x_{i_1}(a_{i_1i_1} - a_{i_3i_1}) + x_{i_3}(a_{i_1i_2} - a_{i_3i_2}) + \cdots + x_{i_m}(a_{i_1i_m} - a_{i_3i_m}) = \dfrac{a_{i_1i_1} - a_{i_3i_3}}{N}, \\ \vdots \qquad\qquad \vdots \qquad\qquad \vdots \\ x_{i_1}(a_{i_1i_1} - a_{i_mi_1}) + x_{i_2}(a_{i_1i_2} - a_{i_mi_2}) + \cdots + x_{i_m}(a_{i_1i_m} - a_{i_mi_m}) = \dfrac{a_{i_1i_1} - a_{i_mi_m}}{N}, \\ x_{i_1} + \qquad x_{i_2} + \cdots + \qquad x_{i_m} = 1, \end{cases} \tag{22}$$

where $0 < x_{i_k} < 1, \forall i_k \in \mathcal{I}$. These equations can also be rewritten in the matrix form

$$\mathbf{A}_{\mathcal{I}}\mathbf{x}_{\mathcal{I}} = \mathbf{b}_{\mathcal{I}}, \tag{23}$$

where

$$\mathbf{A}_{\mathcal{I}} = \begin{pmatrix} a_{i_1i_1} - a_{i_2i_1} & a_{i_1i_2} - a_{i_2i_2} & \cdots & a_{i_1i_m} - a_{i_2i_m} \\ a_{i_1i_1} - a_{i_3i_1} & a_{i_1i_2} - a_{i_3i_2} & \cdots & a_{i_1i_m} - a_{i_3i_m} \\ \vdots & \vdots & \ddots & \vdots \\ a_{i_1i_1} - a_{i_mi_1} & a_{i_1i_2} - a_{i_mi_2} & \cdots & a_{i_1i_m} - a_{i_mi_m} \\ 1 & 1 & \cdots & 1 \end{pmatrix}, \tag{24}$$

$$\mathbf{b}_{\mathcal{I}} = \begin{pmatrix} (a_{i_1i_1} - a_{i_2i_2})/N \\ (a_{i_1i_1} - a_{i_3i_3})/N \\ \vdots \\ (a_{i_1i_1} - a_{i_mi_m})/N \\ 1 \end{pmatrix}. \tag{25}$$

Therefore, if $|\mathbf{A}_{\mathcal{I}}| \neq 0$ holds, there may exist an interior equilibrium point. According to Cramer's rule, we obtain the following equations

$$\begin{aligned} x_{i_1} &= \frac{|\mathbf{A}_{\mathcal{I}1}|}{|\mathbf{A}_{\mathcal{I}}|}, \\ x_{i_2} &= \frac{|\mathbf{A}_{\mathcal{I}2}|}{|\mathbf{A}_{\mathcal{I}}|}, \\ &\vdots \\ x_{i_m} &= \frac{|\mathbf{A}_{\mathcal{I}m}|}{|\mathbf{A}_{\mathcal{I}}|}, \end{aligned} \tag{26}$$

where $\mathbf{A}_{\mathcal{I}k}$ is the matrix formed by replacing the k_{th} column of $\mathbf{A}_{\mathcal{I}}$ by the column vector $\mathbf{b}_{\mathcal{I}}$.

Note that we may get some equilibrium points where there exist negative elements. Therefore, we should check the results after solving the equations.

Stability

Define $f_i(\mathbf{x}) = x_i(\bar{U}_i - \bar{U})$. Obviously, $\dot{f}_i$ and $\ddot{x}_i$ have the same sign. So we can use $f_i(\mathbf{x})$ to analyze the stability of the system. We rewrite Eq. 1 and Eq. 2 in the following form

$$\bar{U}_i = \frac{N}{N-1} \sum_{j=1}^{n} a_{ij} \left(x_j - \frac{1}{N} \delta_{ij} \right), \tag{27}$$

$$\bar{U} = \frac{N}{N-1} \sum_{k=1}^{n} \sum_{j=1}^{n} a_{ij} \left(x_j - \frac{1}{N} \delta_{ij} \right) x_k, \tag{28}$$

from which we get

$$\begin{aligned} \frac{\partial \left(\bar{U}_i - \bar{U} \right)}{\partial x_m} &= \frac{N}{N-1} a_{im} - \frac{N}{N-1} \sum_{j \neq m} a_{mj} x_j - \frac{N}{N-1} \sum_{k \neq m} a_{km} x_k - \frac{N}{N-1} a_{mm} \left(2x_m - \frac{1}{N} \right) \\ &= \frac{N}{N-1} a_{im} - \frac{N}{N-1} \sum_{k=1}^{n} (a_{km} + a_{mk}) x_k + \frac{1}{N-1} a_{mm}. \end{aligned} \tag{29}$$

Thus, we obtain

$$\frac{\partial f_i(\mathbf{x})}{\partial x_m} = \frac{N}{N-1} \left(a_{im} + \frac{1}{N} a_{mm} - \sum_{k=1}^{n} x_k (a_{km} + a_{mk}) \right) x_i + \delta_{im} \left(\bar{U}_i - \bar{U} \right), \tag{30}$$

where $\delta_{im} = 1$ if $i = m$ otherwise $\delta_{im} = 0$. Define the Jacobian matrix

$$\mathbf{J}(\mathbf{x}) = \begin{pmatrix} \frac{\partial f_1(\mathbf{x})}{\partial x_1} & \frac{\partial f_1(\mathbf{x})}{\partial x_2} & \cdots & \frac{\partial f_1(\mathbf{x})}{\partial x_n} \\ \frac{\partial f_2(\mathbf{x})}{\partial x_1} & \frac{\partial f_2(\mathbf{x})}{\partial x_2} & \cdots & \frac{\partial f_2(\mathbf{x})}{\partial x_n} \\ \vdots & \vdots & \ddots & \vdots \\ \frac{\partial f_n(\mathbf{x})}{\partial x_1} & \frac{\partial f_n(\mathbf{x})}{\partial x_2} & \cdots & \frac{\partial f_n(\mathbf{x})}{\partial x_n} \end{pmatrix}. \tag{31}$$

For a given equilibrium point $\mathbf{x}^*$, it is stable if and only if all elements of $\mathbf{J}(\mathbf{x})$ are negative.

Two Steps Ago (Opponent)	Two Steps Ago (Self)	One Step Ago (Opponent)	One Step Ago (Self)	Strategy Choice
Cooperate	Cooperate	Cooperate	Cooperate	Cooperate
Cooperate	Cooperate	Cooperate	Defect	Cooperate
Cooperate	Cooperate	Defect	Cooperate	Defect
Cooperate	Cooperate	Defect	Defect	Defect
Cooperate	Defect	Cooperate	Cooperate	Cooperate
Cooperate	Defect	Cooperate	Defect	Cooperate
Cooperate	Defect	Defect	Cooperate	Defect
Cooperate	Defect	Defect	Defect	Defect
Defect	Cooperate	Cooperate	Cooperate	Cooperate
Defect	Cooperate	Cooperate	Defect	Cooperate
Defect	Cooperate	Defect	Cooperate	Defect
Defect	Cooperate	Defect	Defect	Defect
Defect	Defect	Cooperate	Cooperate	Cooperate
Defect	Defect	Cooperate	Defect	Cooperate
Defect	Defect	Defect	Cooperate	Defect
Defect	Defect	Defect	Defect	Cooperate
-	-	Cooperate	Cooperate	Cooperate
-	-	Cooperate	Defect	Cooperate
-	-	Defect	Cooperate	Cooperate
-	-	Defect	Defect	Defect

Supplementary Table 1: The detailed formulation of MTBR. This table presents the complete decision-making logic of the MTBR strategy based on the last two interactions. Each row represents a unique state, with the first 16 rows showing all possible combinations of full two-step memory, and the last 4 rows representing states with incomplete memory (initial rounds). The 'Strategy Choice' column indicates the MTBR agent's action (Cooperate or Defect) for each state. This shows how MTBR considers both players' actions over two steps to make decisions, illustrating its sophisticated approach to reciprocity and cooperation in iterated games.

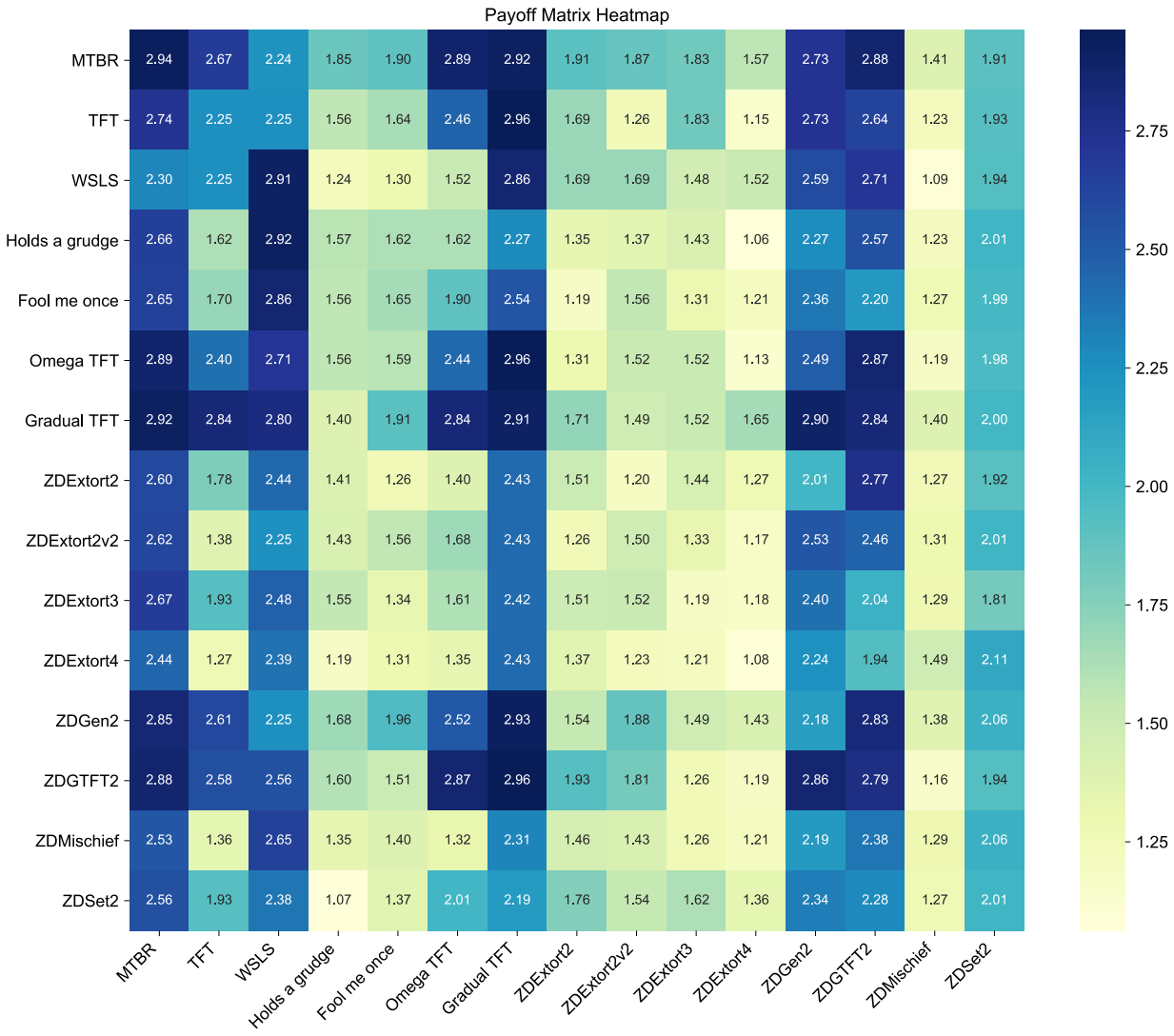

Supplementary Figure 1: Payoff matrix for strategy interactions in the iterated Prisoner's Dilemma. The heatmap shows the average payoffs obtained by 15 different strategies (listed on the x and y axes) when interacting with each other over 20 rounds of the iterated Prisoner's Dilemma. Each cell represents the average payoff of the row strategy when interacting with the column strategy. The color intensity represents the magnitude of the payoff, with darker colors indicating higher payoffs. The payoff structure is defined by the reward matrix [$R = 3$, $T = 5$, $S = 0$, $P = 1$], where R represents the reward for mutual cooperation, T the temptation payoff for defecting while the other cooperates, S the sucker's payoff for cooperating while the other defects, and P the punishment for mutual defection. Strategies include MTBR, TFT, WSLS, Holds a Grudge, Fool me Once, Omega TFT, Gradual TFT, ZDExtort2, ZDExtort2v2, ZDExtort3, ZDExtort4, ZDGen2, ZDGTFT2, ZDMischief, and ZDSet2. MTBR, our proposed strategy, is represented in the first row and column, allowing for direct comparison with other well-established strategies. The heatmap reveals patterns of strategy performance, showcasing how certain strategies, particularly MTBR, can consistently achieve higher payoffs across various interactions, while others may be more vulnerable to exploitation or perform well only against specific opponents.

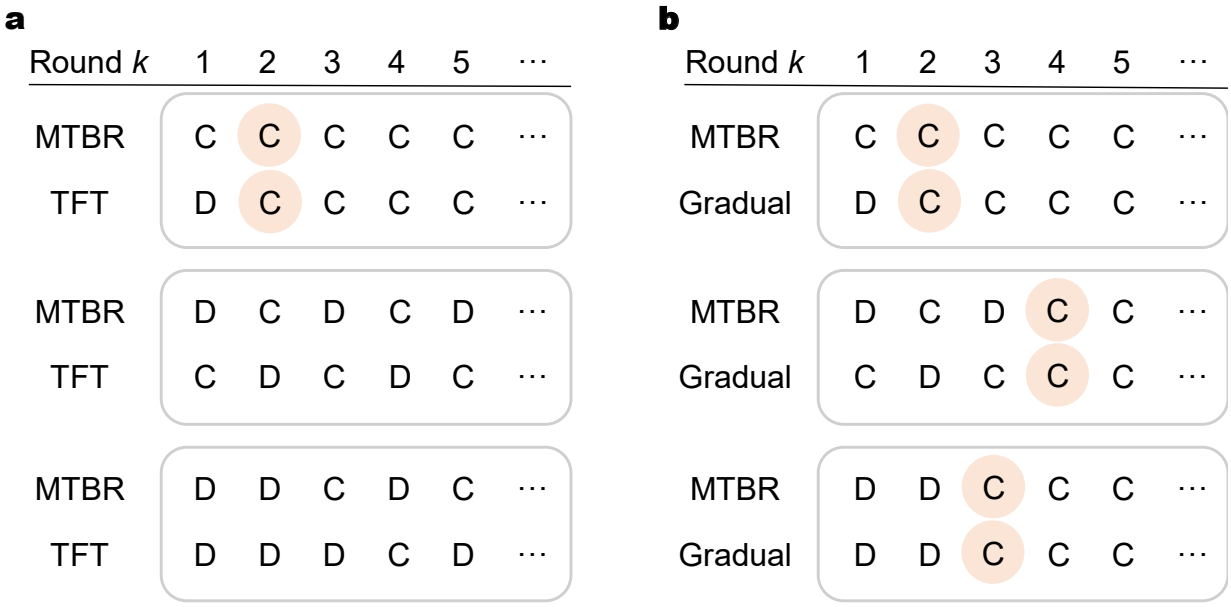

Supplementary Figure 2: Interactions between MTBR, TFT, and GradualTFT in the repeated Prisoner's Dilemma. Panel **a,** Interactions between MTBR and TFT. When MTBR initiates cooperation and TFT defects, MTBR reciprocates cooperatively, leading to mutual cooperation. When MTBR starts with defection and TFT cooperates, they enter a "cooperate-defect" cycle. If both defect initially, MTBR's subsequent cooperation improves the situation to a "cooperate-defect" cycle. This demonstrates MTBR's effectiveness in fostering cooperation when paired with TFT. Panel **b,** Interactions between MTBR and GradualTFT. When MTBR cooperates first and GradualTFT defects, they immediately achieve mutual cooperation. If MTBR defects first while GradualTFT cooperates, mutual cooperation is reached after the third round. When both initially defect, they achieve mutual cooperation after two rounds of goodwill gestures. Yellow circles indicate individuals ceasing defection and entering mutual cooperation. Comparison with panel **a** shows that MTBR and GradualTFT, as cooperative strategies, achieve better mutual cooperation, gaining an advantage in evolutionary games. This figure extends the analysis presented in Fig. 2, providing deeper insights into MTBR's interactions with other strategies in the repeated Prisoner's Dilemma.

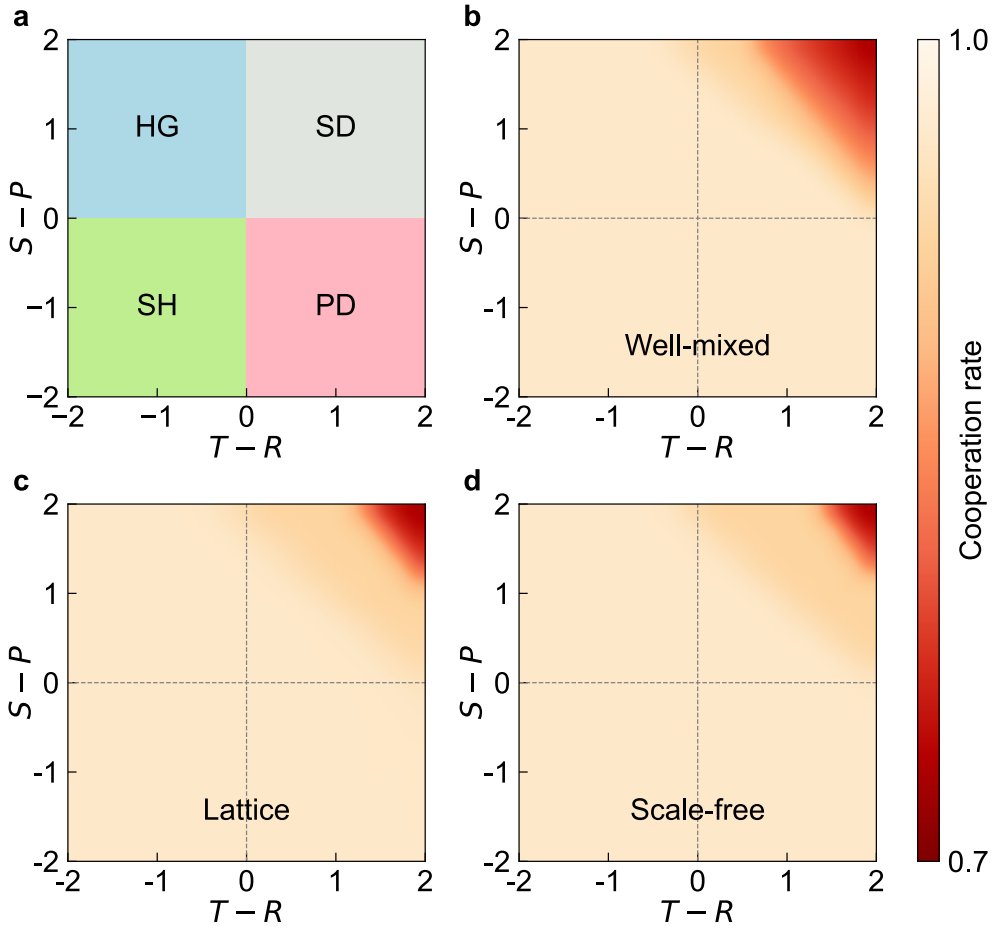

Supplementary Figure 3: Population cooperation rate in evolutionarily stable states under various network structures and payoff matrices. Panel **a** depicts the positioning of four different game types in parameter space, where Greedy ($T - R$) is on the x-axis and Unfearful ($S - P$) is on the y-axis. Each colored block in panels **b**, **c**, and **d** illustrates the population cooperation rate in evolutionarily stable states within a well-mixed population, lattice grid network, and scale-free network, respectively, under different payoff matrices ($R = 3, P = 1$). The color gradient, shifting from yellow to green to dark blue, represents the decline of population cooperation rate from 1.0 to 0.7 in evolutionarily stable states, with T on the x-axis and S on the y-axis. In the study of games under complex network structures, understanding the population cooperation rate is crucial. We observe that near the line $2R = T + S$, the population cooperation rate remains close to 1. Lower population cooperation rates occur in regions where the values of S and T are both higher. Our simulation verification shows that near the line $2R = T + S$, the population exhibits a mixed state of GTFT0.3 and GradualTFT. However, in the region further to the upper right where $2R < T + S$, the population becomes a mixture of MTBR and TFT. Due to the strong cooperative tendency of GTFT0.3 and GradualTFT, the population cooperation rate also approaches 1 near the line $2R = T + S$. In the region where $2R < T + S$, as the proportion of TFT in the population increases, the population cooperation rate gradually decreases to around 0.7.

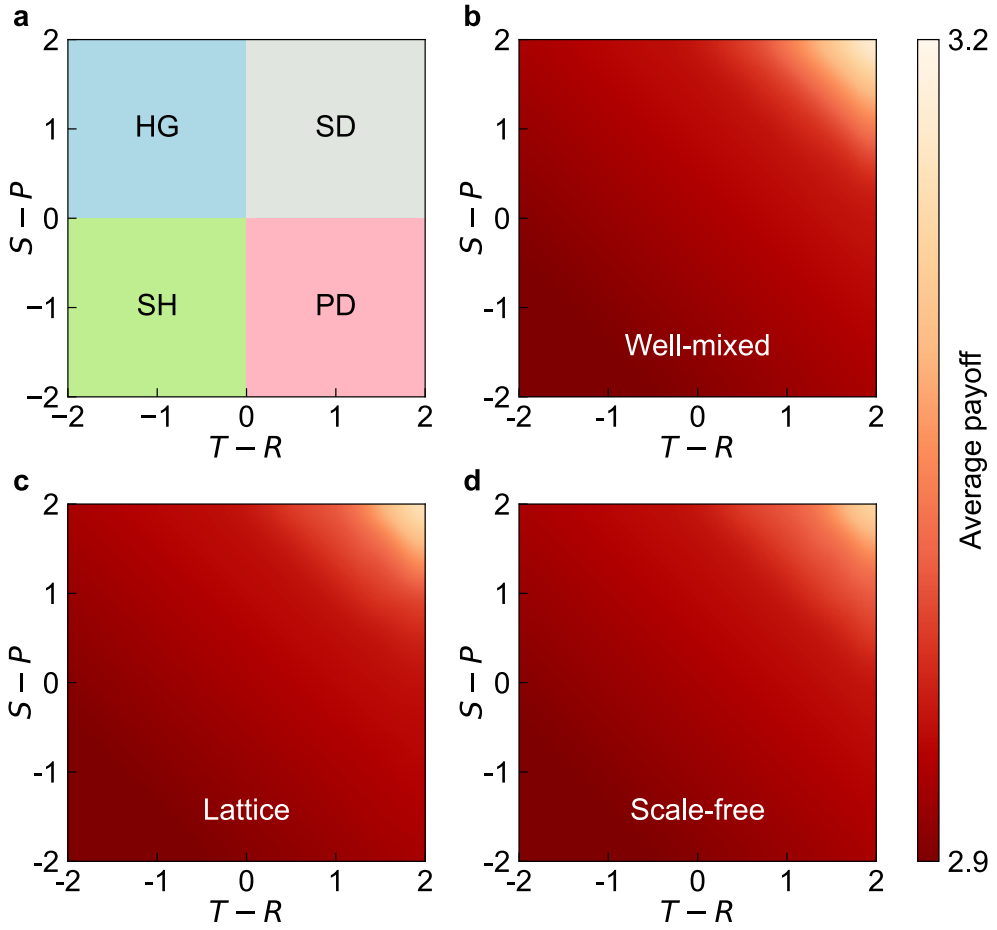

Supplementary Figure 4: Average payoff in evolutionarily stable states under various network structures and payoff matrices. Panel **a** depicts the positioning of four different game types in parameter space, where Greedy ($T - R$) is on the x-axis and Unfearful ($S - P$) is on the y-axis. Each colored block in panels **b**, **c**, and **d** illustrates the average payoff in evolutionarily stable states within a well-mixed population, lattice grid network, and scale-free network, respectively, under different payoff matrices ($R = 3, P = 1$). The color gradient, shifting from yellow to green to dark blue, represents the decline of average payoff from 3.2 to 2.9 in evolutionarily stable states, with T on the x-axis and S on the y-axis. In addition to population cooperation rate, we also focus on another important metric - the average payoff of all individuals in the population. We found that the trend of average payoff changes is completely opposite to that of the Population Cooperation Rate. The reason is that when $2R < T + S$, both individuals obtaining cooperation and defection behaviors will achieve higher payoffs than mutual cooperation. In this region, the payoff of mutual cooperation is not as good as the stable "cooperate-defect, defect-cooperate" cycle. This also explains the equilibrium reached between MTBR and TFT in this region - when identical individuals meet, TFT gains higher payoff when they randomly choose "cooperate" and "defect" in the first round (see Fig. 2a), and MTBR gains higher payoff when both sides randomly defect in the first round (see Fig. 2b). This interplay explains the strategic variations, highlighting the complexity of interactions and outcomes within these game settings.

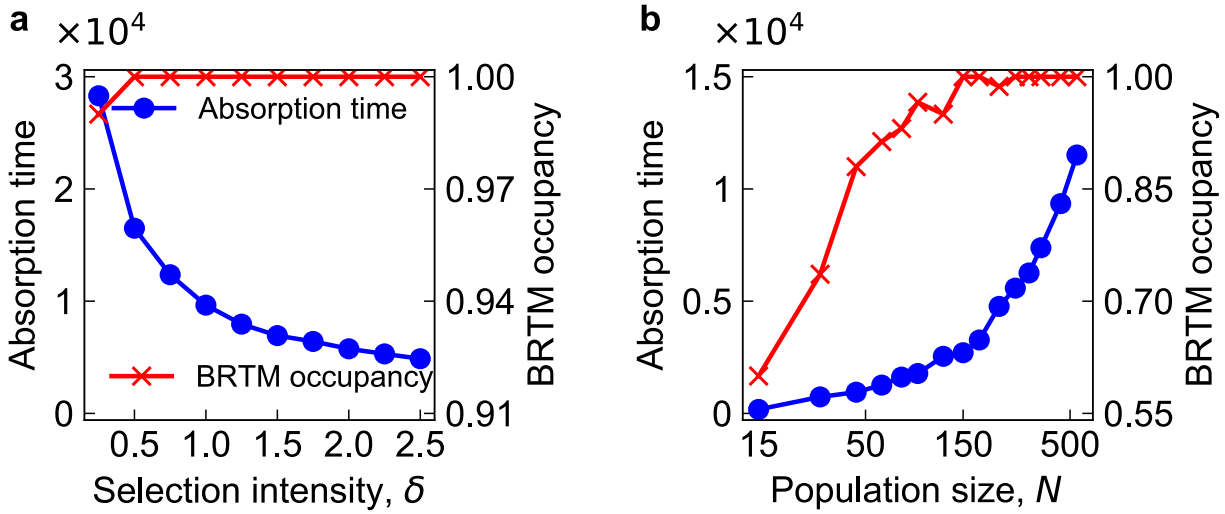

Supplementary Figure 5: Impact of selection intensity and population size on evolutionary dynamics. The blue lines marked with dots represent the absorption time (generations) required for the population to reach evolutionarily stable states. The red lines marked with "x" symbols represent the fraction of the population occupied by MTBR in evolutionarily stable states. Panel **a** illustrates the influence of selection intensity s on the absorption time and the occupancy probability of MTBR in evolutionarily stable states for a fixed population size of $N = 500$. As selection intensity increases, we observe a corresponding decrease in absorption time. Notably, at $N = 500$, MTBR demonstrates the ability to stably occupy the population. Panel **b** demonstrates the impact of population size N on the absorption time and the occupancy probability of MTBR in evolutionarily stable states for a fixed selection intensity of $\delta = 1$. Larger population sizes result in slower strategy dissemination and longer absorption times. In smaller populations, exploitative strategies have a competitive advantage. As the population size increases, the high returns resulting from interactions between cooperative strategies gradually emerge. All data points represent the average of over 100 repeated experiments.

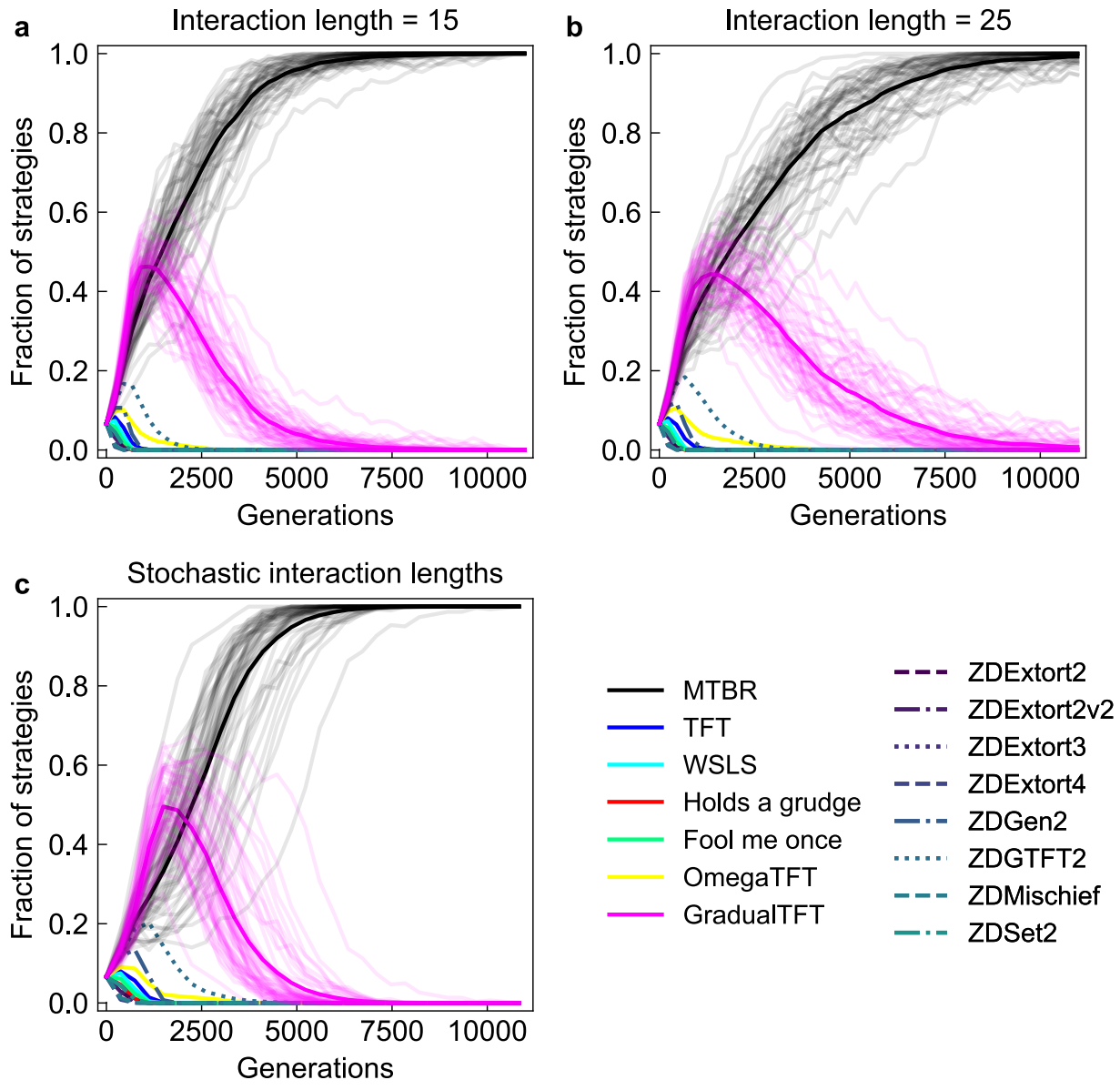

Supplementary Figure 6: Impact of interaction length on the evolution of strategies. The figure shows the evolutionary dynamics of strategies under different interaction lengths: 15 rounds (panel **a**), 25 rounds (panel **b**), and stochastic length with an average of 20 rounds (panel **c**). Each line represents the proportion of a specific strategy in the population over time. Although the discovery of MTBR is based on a setup of twenty rounds, we have considered a variety of interaction setups, including shorter and longer interaction lengths, as well as stochastic interaction lengths. The stochastic interaction lengths experiment involves a 5% probability of terminating the game after each round, resulting in a mathematical expectation of 20 rounds. We found that the interaction length only slightly affects the speed of evolution within the population, without altering the final evolutionary outcomes. The similarity in evolutionary trajectories across different interaction lengths demonstrates the robustness of MTBR's evolutionary advantages.